Proceedings World Geothermal Congress 2015
Melbourne, Australia, 19-25 April 2015

Reservoir Simulation for Reinjected Water Return in Produced Fluid of Wells at Ogiri Geothermal Field, Japan

Shunichi HIRAYAMA, Ryuichi ITOI, Toshiaki TANAKA, Junichi TAKAYAMA

Department of Earth Resources Engineering, Kyushu University, 744 Motooka, Nishiku, Fukuoka, 819-0395, Japan

s-hirayama@mine.kyushu-u.ac.jp

Keywords: Reservoir simulation, reinjection, numerical model, Ogiri geothermal field

ABSTRACT

Numerical simulations of the Ogiri geothermal field were conducted using a fractured model for evaluating return of reinjected water to production wells. In this study, a MINC method was applied to grid blocks both in production and reinjection zones to describe the return of reinjected water in the reservoir. A mixing ratio of reinjected water to the produced fluid at respective production wells were quantitatively evaluated by using a function of two kinds of waters built in the TOUGH2 numerical simulator.

1. INTRODUCTION

Reinjecting water back into a formation is a useful technique of recharging fluid into a reservoir. Reinjected water is heated as it flows in the formation towards the production zone. However, excessive and quick return of reinjected water to the production zone causes cooling, and consequently decreases in steam production of wells. It is then necessary to properly manage the reinjection scheme for a sustainable development of the field.

Reservoir simulations provide visualization of the condition of the reservoir systems based on measured field data. Itoi et al. (2011) conducted a reservoir simulation of reinjected-water return at the Ogiri geothermal field using a three-dimensional reservoir model. The model included a grid system applied with a MINC method (Pruess et al., 1999), which was only for the shallow production zone, and the grids in other domain in the model were of porous type.

In this study, we assigned grids with the MINC method to the other domains of fault zone and reinjection zone and carried out reservoir simulations using TOUGH2 (Pruess et al., 1999) to quantify mass ratios of reinjected water to produced fluid of wells. The temporal change of mass ratio of reinjected water from respective reinjection wells was analyzed.

2. OGIRI GEOTHERMAL FIELD

The Ogiri geothermal field is located in Kagoshima-prefecture, southern Kyushu, Japan at an elevation of about 800 m a.s.l (above sea level). The field has been developed by Nittetsu Mining Co. and the power plant has been operated by Kyushu Electric Co. The Ogiri geothermal power plant started its operation in March 1996 with an installed capacity of 30 MW. Goko (2000) conducted geothermal and geochemical studies on the system of Ogiri. Figure 1 shows a conceptual model of the Ogiri geothermal system with fault zones, and flow directions of high temperature fluid and reinjected water were estimated. Subsurface temperature distribution in west Ogiri indicates that the temperature increases from northwest to southeast. This implies that the heat source charging the area lies to the southeast of Ogiri, below the Kirishima volcanoes. In Ogiri, production wells were mainly drilled along the Ginyu fault which is the main reservoir in the Ogiri geothermal field. Reinjection wells are located in the western part of the field whereas production wells are in the eastern part. Vertical temperature profiles of wells indicate that the Ginyu fault has

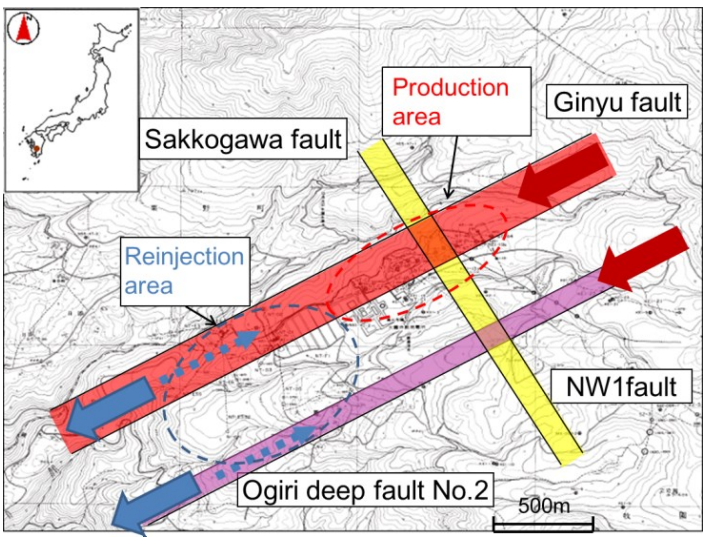

Figure 1: Conceptual model of Ogiri geothermal field. Red and blue arrows indicate estimated flow directions of high temperature fluid and reinjected water.

uniform temperature distribution of 230 to 232 °C at depths below 0m a.s.l. There is a low permeability rock in the shallow zone, of which vertical thickness is 200 – 400 m and in which temperature is from 50 to 130 °C. This low permeability rock plays as cap rock, which prevents from low temperature water flowing into a reservoir.

3. THREE DIMENSIONAL NUMERICAL MODEL

A numerical model of the Ogiri geothermal reservoir had a three-dimensional grid system which covered an area of 5.5 km × 3.9 km with elevations of 230m a.s.l down to -2600m a.s.l. The grid block size varied from 100 m ×100 m to 1000 m × 1000 m and the thickness of layers ranged from 50 m to 1600 m. The horizontal plain was divided into 23 blocks from east to west and 13 blocks from south to north. Vertical domain was divided into 13 layers. The total number of grid in this model was 3887. The top layer to the bottom layer were named AA, and LL. The grid system was tilted by 27° from east to north to represent properly the main fault system in ENE-SWS directions in rectangular coordinates. Figure 2 shows the grid system used in the model with feed point location of wells.

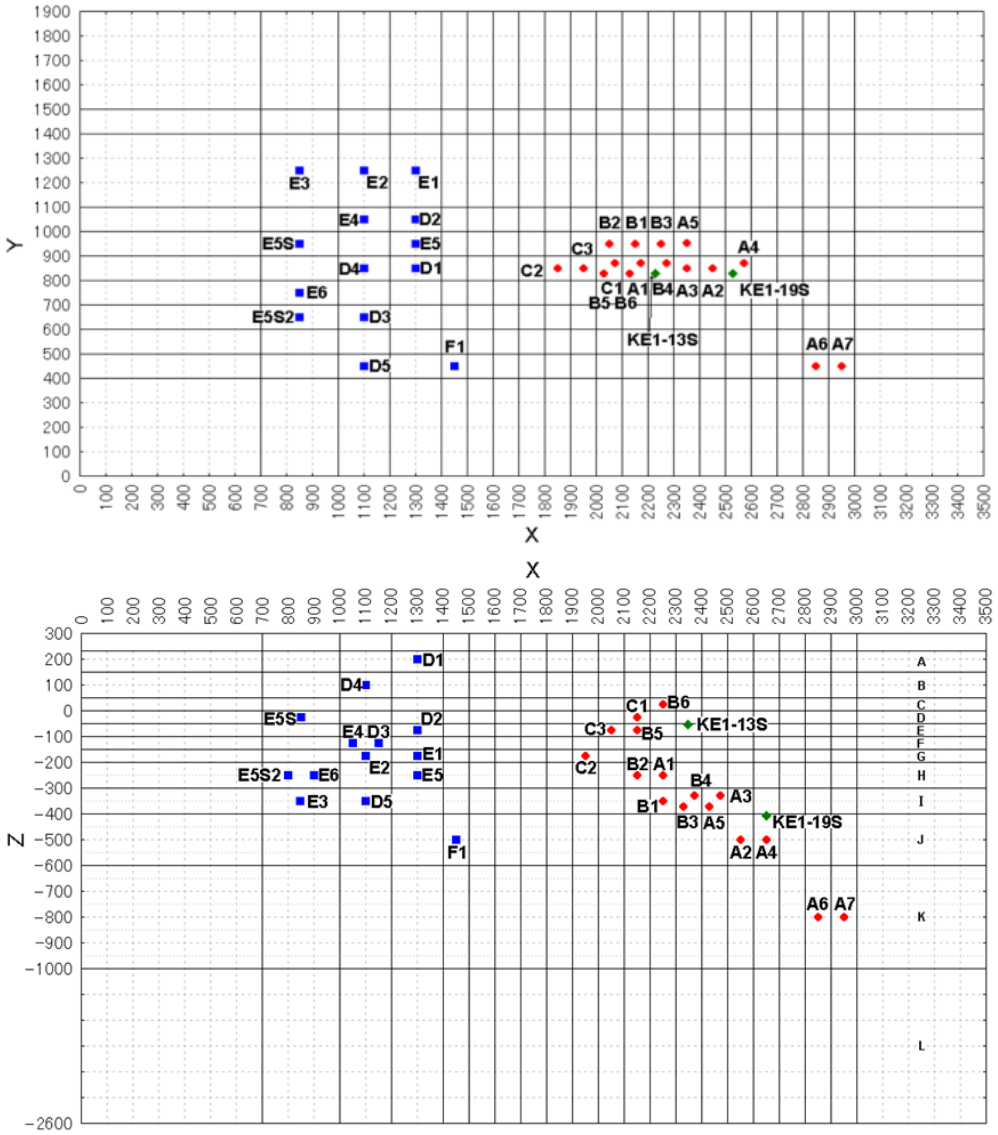

Figure 2: Grid system with feed point location of wells. Peripheral grid blocks are not shown.

We applied the MINC method (Pruess et al., 1999) to the grid blocks in the fault zones and the reinjection zone: the Ginyu fault, the Ogiri deep fault No.2, the NW fault, and the reinjection area. Figure 3 shows the zones in the model where MINC method is implemented, indicated by colored grid. The MINC method is applicable to processes of fluid and heat exchange between fracture and unfractured rock, which occur in production and reinjection operation in fractured geothermal reservoirs. In the MINC model, the grid is divided into fracture and matrix parts. The fracture parts have high permeability and porosity, while the matrix parts have low permeability and porosity. Thus, global fluid flow only occurs in fractured zones. Thermodynamic conditions in matrix are controlled by its distance from the fracture.

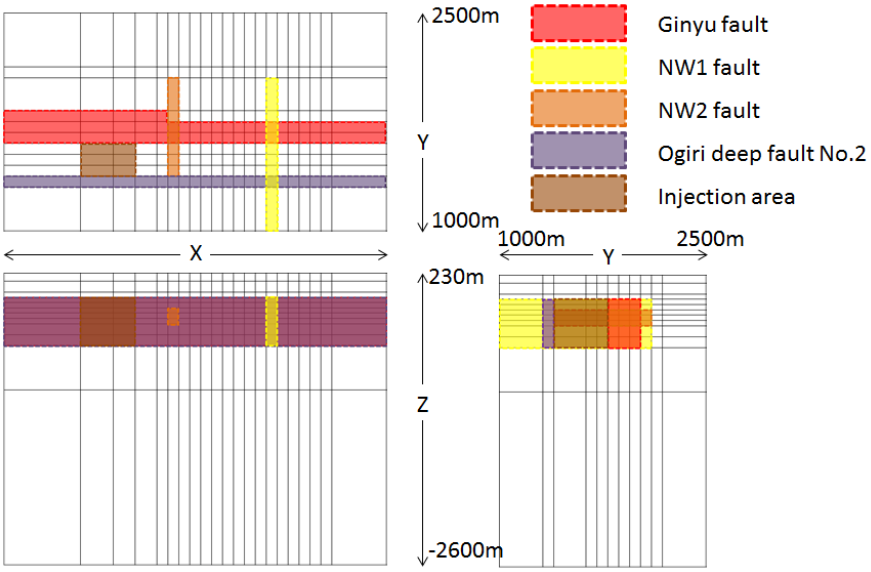

Figure 3: Colored grid applied with MINC method in this model.

4. SIMULATION CONDITIONS AND NATUNAL-STATE SIMULATION

We developed a numerical model using TOUGH2. First, we carried out natural-state simulation to obtain the temperature and pressure distributions of the Ogiri geothermal reservoir before exploitation. In natural-state simulation, we conducted a forward simulation to match simulated results with measured temperature and pressure in exploration wells and observation wells. For initial conditions, a pressure equilibrium condition saturated with water at 75°C was specified. As boundary conditions, constant pressure of 9.807 $\times 10^4$ Pa and temperature of 75°C above the top surface were given. The lateral boundaries were assumed to be impermeable to mass and adiabatic to heat. However, reinjected water flowing out from the domain was realized by assigning productivity index (PI) of 1.0×10^{-13}m^3 to grid blocks in the western most areas in the model. Mass recharge and constant heat flux were set at the bottom layer of the grid system. The mass recharge was specified at two areas: 40kg/s of 1061kJ/kg (245°C) and 20kg/s of 1061kJ/kg as shown in Figure 4. Two values of heat flux were also given to represent temperature distribution: 0.035W/m^2 in the south-east part of the model and 0.023W/m^2 in the remaining area.

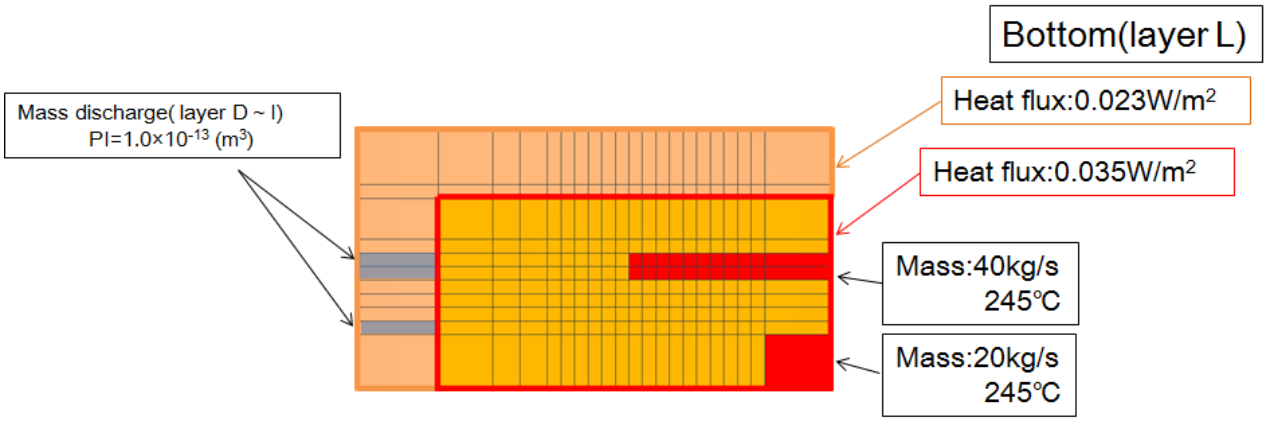

Figure 4: Boundary conditions in bottom layer and mass discharge area.

Figure 5 shows the comparison between measured and simulated temperature profiles for natural-state in two observation wells, KE1-13S and KE1-19S. Both wells are located in the Ginyu fault. The simulated temperature of wells KE1-13S and KE1-19S has good fit with measured temperature below 0m a.s.l. Above 0m a.s.l., however, the simulated temperatures were lower compared to that of the measured one. This is due to the constant temperature of 75°C that was set as boundary condition above the top surface of the grid system. Figure 6 shows the comparison between simulated and measured pressure values at feedzone of wells. The figure shows a good agreement between simulated and measured pressure values.

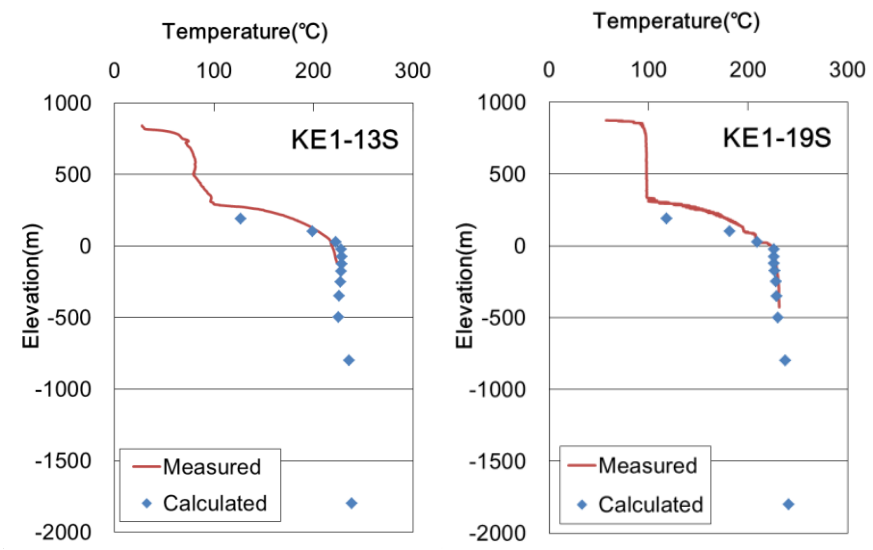

Figure 5: Comparison of simulated and measured temperature in observation wells for natural-state simulation

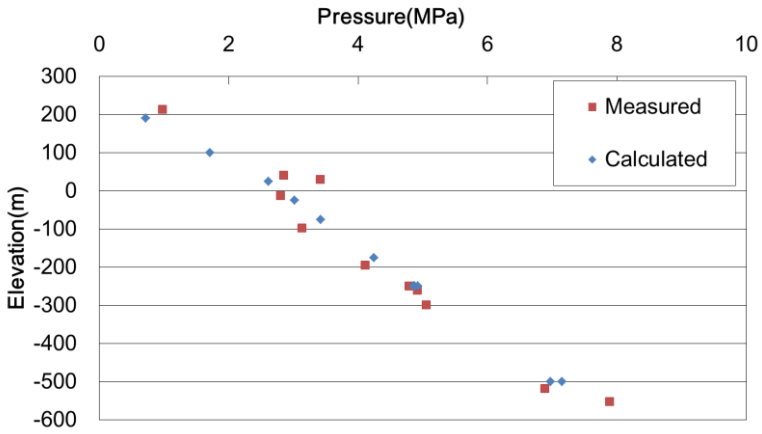

Figure 6: Comparison of simulated and measured pressure at well feedpoints for natural-state simulation

5. MASS FRACTION OF REINJECTED WATER SIMULATION

After natural-state simulation was completed, we carried out history matching simulations using production and reinjection histories since 1995. The calibration period is 29 years from 1996 to 2013. Boundary conditions were set in the same manner as the natural-state simulation. The result of the natural-state simulation on the distributions of temperature and pressure were given as initial conditions for history-matching simulation. Figure 7 shows the measured and simulated pressures in Well KE1-19S with time. The match between the measured and simulated pressure was good throughout the simulation period.

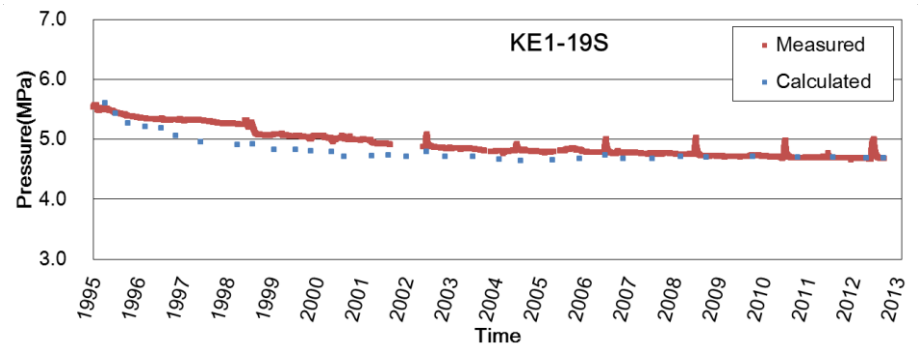

Figure 7: Comparison of simulated pressure and measured one in observation wells

After history matching simulations, numerical analyses for the mass fraction of reinjected water were conducted by adopting a function of two kinds of fluid in TOUGH2. High temperature recharge water was specified as “water 1” whereas reinjected water at a specific well was specified as “water 2”.The simulation was repeated by specifying the reinjected water as “water 2” for each reinjection well. Mass fraction of “water 2” in a grid block, which had a feedpoint of production well, was calculated. Furthermore, the mass ratio of the cumulative mass fraction of “water 2” for all reinjection waters to the produced fluid in the production wells was calculated. The mass ratio of reinjected water to produced fluid at a production well, X (%), is expressed by:

$$X = (M_{water\ 2}/M) \times 100 \quad (1)$$

M is the fluid mass in a grid block where feed zone of production well is located (kg), M_{water2} is the mass of reinjected water labeled as "water 2" in this grid block (kg), respectively. Thus, the results can be used for drawing distribution of X in layers.

Figure 8 shows the mass ratio of reinjected water to produced fluid, X (%), at Well B1. Lower figure presents production history for B1 and reinjection rates at D5 and E6 with time. Dotted line indicates the result of the previous model (Itoi et al., 2011). Value of X with respect to E6 quickly increases with time soon after reinjection started and reaches to 40%. Then, it starts decreasing once the reinjection rate was reduced in 2001. These changes in X with time reflect the change in flow rate at E6 as shown in the lower figure. This is because that B1 is located relatively close to reinjection area (Figure 2), and thus a significant amount of reinjected water into E6 reaches B1. On the other hand, X value of the previous model for E6 slowly increases with time whereas that of the present model quickly increases with time. This difference is due to the expansion of MINC grid system.

Figure 9 shows distributions of X with respect to reinjection wells E6 and D5 in Layer I. The distribution of X for E6 indicates high value in grids corresponding to the Ginyu fault, thus reinjected water of E6 flows along the Ginyu fault to production area. Reinjection well D5 is located in the Ogiri deep fault No.2 and its reinjected water mainly flows eastward along this fault. A part of water also flows in the Ginyu fault. Thus, reinjected water at D5 flows into the Ginyu fault from east and then westward into the production zone.

Figure 10 shows the mass ratio of reinjected water to produced fluid at A2 which is located on the intersection of the Ginyu fault and the NW1 fault. The figure also presents production rate at A2 and reinjection rates at E6 and D5. Figure 10 indicates that X values for the previous model was below 1% for three reinjection wells whereas X values for three reinjection wells quick increase and are higher in the present model. However, return of reinjected water at E6 located in the western area shows smaller value than that at A2 compared with that at B1. This is because A2 is located eastern end of the production area and relatively far from the reinjection area in the western part of Ogiri. In Figure 11, the distribution of X with respect to reinjection well F1 is illustrated. The F1 is located in the Ogiri deep fault No.2, then its reinjected water flows along this fault eastward, then flows northward in the NW1 fault. This then supports the large amount of fluid at F1 occupied in the produced fluid at A2 as shown in Figure 10.

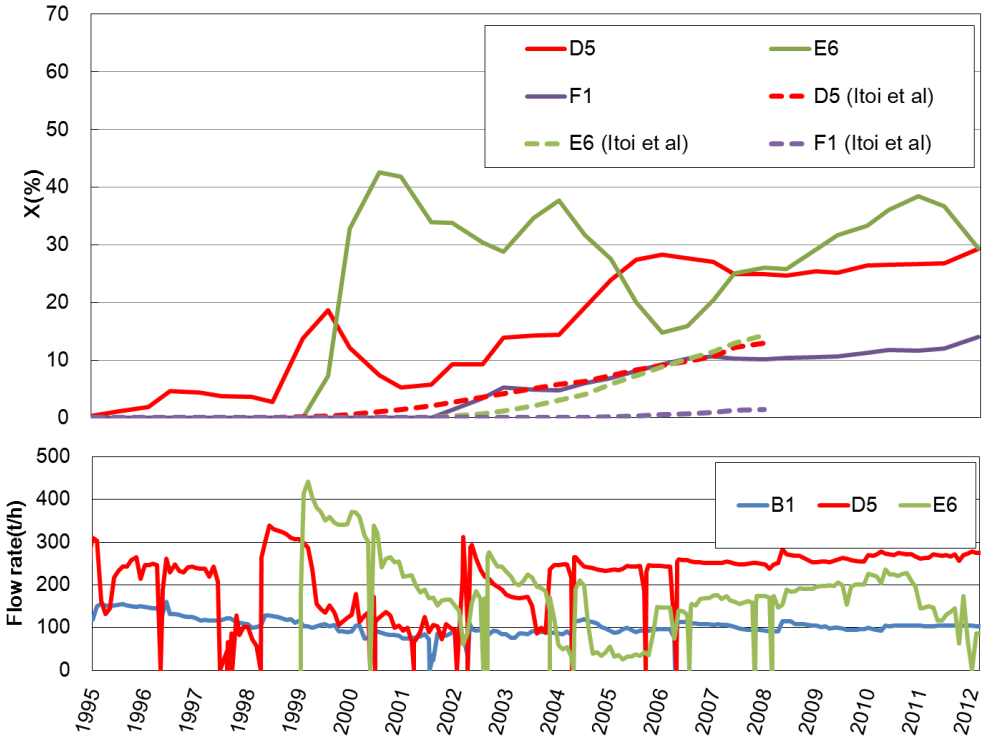

Figure 8: Simulated mass ratio, X, and production rate of Well B1, and reinjection rate of Well E4.

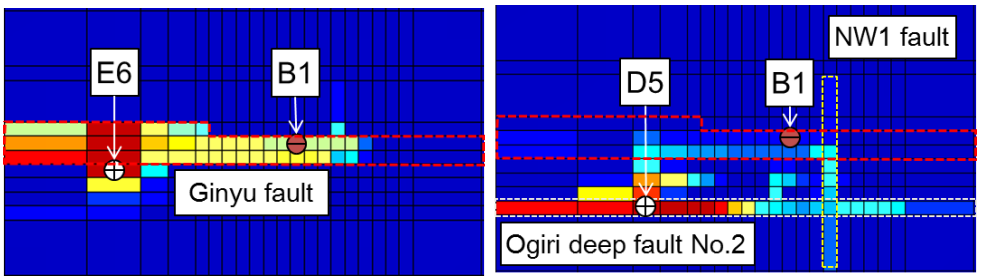

Figure 9: Distributions of X of E6 and D5 in 2002 in Layer I.

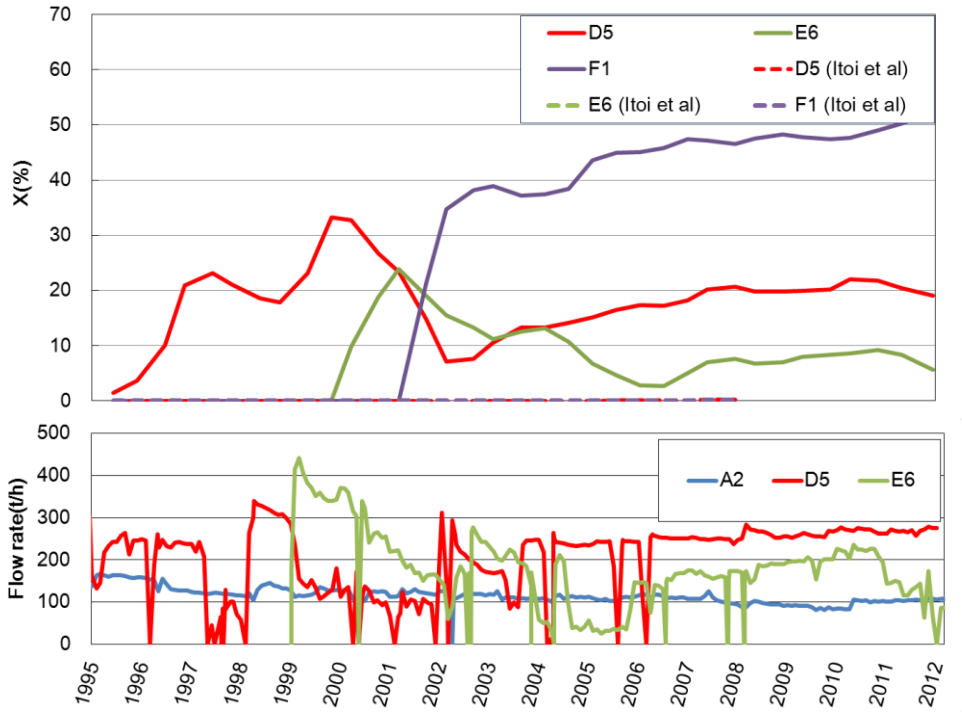

Figure 10: Simulated mass ratio, X, and production rate of Well A2, and reinjection rate of Well E4.

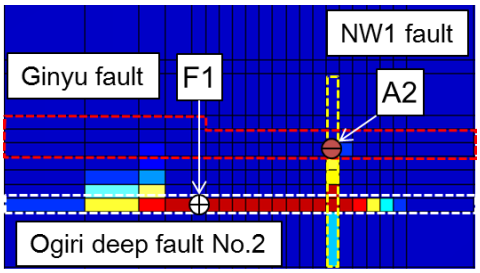

Figure 11: Distributions of X at F1 in 2002 in Layer J

6. CONCLUSION

We conducted numerical simulations for evaluating mass ratio of reinjected water in the produced fluid at the Ogiri geothermal reservoir using a grid model applied with a MINC method to fault zones and reinjection zone. Results are summarized as follows:

1. A good match for the pressure behavior in the observation wells was obtained.

2. Quick return of reinjected water was simulated in the production wells which are located within the same fault zone expressed by MINC grid.

3. Areal distribution of mass ratio in grid blocks indicates the flow of reinjected water in the numerical model.

ACKNOWLEDGEMENT

The authors thank Nittetsu Mining Co., Ltd for support and permission to use the field data.

REFERENCES

Goko, K.: Geological analysis and evaluation of the Ogiri geothermal structure in the Kirishima geothermal area, *Resource Geology, (in Japanese with English abstract)*, **45**, (1995), 41-52.

Goko, K.:Structure and hydrology of the Ogiri field, West Kirishima geothermal area, Kyushu, Japan, *Geothermics*, **29**, (2000), 127-149.

Horikoshi, T., Takayama, J., Takeshita, K., Goko, K., and Yoshizawa, H.:An analysis of the geothermal structure of the Ogiri geothermal field based on the surveys and operational data of the Ogiri Power Station after its commencement, *Resource Geology (in Japanese with English abstract)*, **55**, (2005), 25-38.Japan Geothermal Energy Association(JGEA): Directory of Geothermal Power Plant in Japan (New Edition), *Japan Geothermal Energy Association (in Japanese)*, (2000), 254pp.

Kumamoto, Y., Itoi, R., Tanaka, T., and Hazama, Y.Development of the Optimum Numerical ReservoirModel of the Ogiri Geothermal Field, Kyushu, Japan,

Itoi, R., Yamashita, S., Tanaka, T., Takayama, J.: Numerical Simulation of Reinjected Water Return to Production Wells in Ogiri Geothermal Reservoir, Japan, *Trans. Geothermal Resources Council*, **32**, (2011), 1437-1441.

Pruess, K., Oldenburg, C. and Moridis, G. : TOUGH2 User's Guide, Version 2.0, *Report LBNL-43134*, Earth Sciences Division, Lawrence Berkeley NationalLaboratory, University of California, Berkeley, CA(1999)